

LET THE CODE LLM EDIT ITSELF WHEN YOU EDIT THE CODE

Anonymous authors

Paper under double-blind review

ABSTRACT

In this work, we investigate a typical scenario in code generation where a developer edits existing code in real time and requests a code assistant, e.g., a large language model, to re-predict the next token or next line on the fly. Naively, the LLM needs to re-encode the entire KV cache to provide an accurate prediction. However, this process is computationally expensive, especially when the sequence length is long. Simply encoding the edited subsequence and integrating it to the original KV cache meets the temporal confusion problem, leading to significantly worse performance. We address this efficiency and accuracy trade-off by introducing **Positional Integrity Encoding (PIE)**. Building upon the rotary positional encoding, PIE first removes the rotary matrices in the Key cache that introduce temporal confusion and then reapplies the correct rotary matrices. This process ensures that positional relationships between tokens are correct and requires only a single round of matrix multiplication. We validate the effectiveness of PIE through extensive experiments on the RepoBench-C-8k dataset, utilizing DeepSeek-Coder models with 1.3B, 6.7B, and 33B parameters. Our evaluation includes three real-world coding tasks: code insertion, code deletion, and multi-place code editing. Results demonstrate that PIE reduces computational overhead by over 85% compared to the standard full recomputation approach across all model sizes and tasks while well approximating the model performance.

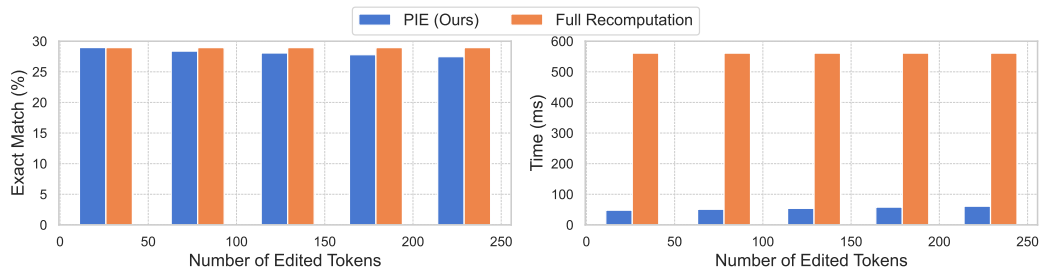


Figure 1: Latency and accuracy comparison of the full recomputation approach and our PIE using DeepSeek-Coder 6.7B on the RepoBench-C-8k(XF-F) Python dataset on a single A100 GPU. The latency only records the time cost for the KV cache update.

1 INTRODUCTION

Large language models (LLMs) (Dettmers et al., 2022; Anil et al., 2023; Touvron et al., 2023; Zeng et al., 2023) have seen widespread adoption and achieved impressive results across various natural language processing (NLP) tasks. Despite these successes, LLMs face significant computational challenges, particularly in handling long sequences. To address this, numerous approaches have been proposed to accelerate the inference process, including lossless (e.g., memory and IO optimization (Dao et al., 2022; Kwon et al., 2023; Sheng et al., 2023), speculative decoding (Stern et al., 2018; Leviathan et al., 2023)) and lossy techniques (e.g., quantization (Frantar et al., 2022; Xiao et al., 2023) and KV cache eviction (Xiao et al., 2024; Zhang et al., 2024)). We refer to the above setting as

054 the *static* setting, where the content is fixed, and the goal is to generate responses efficiently without
055 compromising too much on performance.

056 Besides the static setting, we observe there is a strong demand for an alternative, which we call the
057 *real-time editing* setting, where users frequently edit the content and expect the LLM to generate
058 correct responses based on the updated information. A typical scenario is the interactive coding
059 assistant, where developers often make incremental changes to their existing code and require the AI
060 copilot to correctly predict the next line or complete a partial code snippet on the fly. The standard
061 approach is re-encoding the KV cache of the content after each edit and then making the prediction.
062 However, as illustrated in Figure 1, this approach leads to considerable substantial computational
063 overhead and latency when the content is long (Fu, 2024; Agrawal et al., 2024), making it impractical
064 for real-time applications where quick and accurate responses are essential.

065 In this paper, we aim to improve the efficiency of AI copilots in real-time editing scenarios, as
066 illustrated in Figure 2. Naively, an efficient strategy is encoding only the edited subsequence and then
067 directly integrating those keys and values into the original KV cache. However, this strategy results
068 in temporal confusion between the pre-edit and post-edit sequences. Keys of certain positions either
069 disappear or multiple keys at different positions share the same index, causing the model to attend
070 to incorrect information, leading to poor next-token prediction performance in practice. To address
071 this problem, we introduce **Positional Integrity Encoding (PIE)**. PIE is built upon rotary positional
072 encoding (RoPE) (Su et al., 2021), the de-facto standard component in modern LLMs. PIE first
073 removes the rotary matrices in the Key cache that introduce temporal confusion and then reapplies
074 the correct rotary matrix for each position through simple matrix multiplications. By ensuring that
075 the positional relationships between tokens in the new sequence are unique and consecutive, PIE can
076 help the model make accurate predictions. It is worth noting that the calculation of PIE requires only
077 a single round of matrix operations to modify the KV cache, resulting in negligible computational
078 overhead.

079 We demonstrate the effectiveness of Positional Integrity Encoding (PIE) through extensive experi-
080 ments conducted on the RepoBench-C-8k dataset, utilizing the DeepSeek-Coder (Guo et al., 2024)
081 models with 1.3B, 6.7B, and 33B parameters. To rigorously evaluate PIE’s performance, we curated
082 three tasks designed to simulate real-world coding scenarios: code insertion, code deletion, and
083 multi-place code edition. These tasks were chosen to reflect common operations that developers
084 perform during interactive coding sessions, thereby providing a comprehensive assessment of PIE’s
085 practical utility. Our experimental results indicate that PIE achieves a reduction in computational
086 overhead of over 85% for editing the KV cache across all model sizes and tasks without compromising
087 performance compared to the naive full-recomputation approach. By leveraging PIE, developers can
088 experience efficient interactions with AI coding assistants.

090 2 RELATED WORK

093 **Positional Encodings** Positional information is essential for modeling languages. The original
094 Transformer model (Vaswani et al., 2017) encodes positional information using Absolute Positional
095 Encoding (APE). In particular, a (learnable) real-valued embedding is assigned to each position i .
096 Differently, Relative Positional Encodings (RPE) (Shaw et al., 2018; Dai et al., 2019; Raffel et al.,
097 2020; Press et al., 2022; Su et al., 2021; Luo et al., 2021; 2022; Chi et al., 2022; Sun et al., 2023;
098 Chi et al., 2023; Li et al., 2023; He et al., 2024) instead encode the relative distance $i - j$ for each
099 position pair (i, j) . One of the most widely used RPE in state-of-the-art LLMs is Rotary Position
100 Encoding (RoPE) (Su et al., 2021). RoPE rotates the query and key vectors by an angle proportional
101 to their absolute positions before the attention mechanism, resulting in the attention being a function
102 of the relative distance between tokens.

103 In the literature, relative positional encodings play essential roles across various tasks and data
104 modalities, such as improving the length extrapolation capability of language models (Press et al.,
105 2022; Sun et al., 2023; Chi et al., 2022; 2023; He et al., 2024) and enabling flexible modeling of
106 structural information beyond sequence data like images (Liu et al., 2021) and graphs (Ying et al.,
107 2021; Zhang et al., 2023a; Luo et al., 2023). In this work, we develop the Positional Integrity
Encoding based on RoPE to improve the efficiency of LLMs in the real-time editing setting.

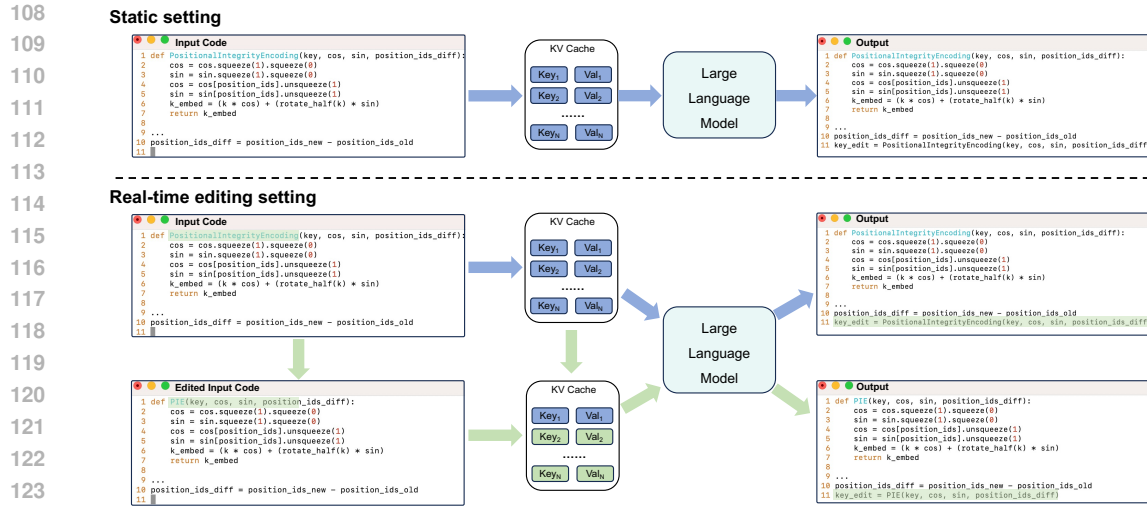


Figure 2: Illustration of the KV cache mechanism in both static and real-time editing settings for large language models (LLMs). **Top:** In the static setting, the model processes a fixed input to generate predictions, leveraging precomputed Key/Value (KV) pairs stored in the cache. **Bottom:** In the real-time editing setting, the input code is frequently edited, necessitating updates to the KV cache to maintain accurate information to generate the correct next tokens. Our objective is to optimize the efficiency of the green arrow pathway, which represents the process of updating the KV cache in response to code edits.

Transformer Efficiency Improving the efficiency of Transformer models has great significance in real-world applications. In the literature, existing approaches can be briefly categorized into (1) efficient attention, (2) model compression, and (3) system-architecture co-design.

The attention module of Transformer needs to calculate pairwise correlations between all positions, resulting in quadratic time and memory cost with respect to the sequence length. To reduce the cost, many efficient attention variants have been proposed, such as (1) sparse attentions (Child et al., 2019; Beltagy et al., 2020; Qiu et al., 2020), which design either pre-defined or learnable patterns to reduce the amount of the key-value pairs that each query needs to attend to; (2) approximation-based attention (Katharopoulos et al., 2020; Wang et al., 2020; Choromanski et al., 2021; Kitaev et al., 2020; Tay et al., 2020; Roy et al., 2021), which use tailored approaches like low-rank projection or random features to approximate standard attention for efficient computation.

Another perspective for Transformer efficiency is model compression, mainly including (1) pruning (Wang et al., 2021; Hubara et al., 2021; Ma et al., 2023; Frantar & Alistarh, 2023), which aims at removing redundant model parameters or layers for efficient deployment without scarifying performance; (2) quantization (Yao et al., 2022; Park et al., 2022; Dettmers et al., 2022; Frantar et al., 2022; Xiao et al., 2023; Liu et al., 2023), which uses post-processing to represent weights and activations via low-precision format for reducing time and memory costs; (3) knowledge distillation (Sanh et al., 2019; Gu et al., 2024), which uses a smaller model to learn knowledge from a large model for balancing efficiency-accuracy trade-offs.

In the era of LLMs, the importance of system-architecture co-design has been highlighted to improve Transformer efficiency further. Many works begin to design more efficient approaches for serving Transformers regarding the characteristics of computer systems for real-world applications, such as FlashAttention (Dao et al., 2022; Dao, 2023), PagedAttention (Kwon et al., 2023), and FlexGen (Sheng et al., 2023) that are proposed for memory and I/O optimization. Additionally, to reduce functional calls during generation, speculative decoding (Stern et al., 2018; Leviathan et al., 2023; Chen et al., 2023; Miao et al., 2023; Spector & Re, 2023; Cai et al., 2024; Zhang et al., 2023b; He et al., 2023; Li et al., 2024) has been proposed. Our Positional Integrity Encoding is specially designed to improve the efficiency of LLMs in real-time editing settings, which can be seamlessly combined with all the above-introduced approaches to achieve further speed-ups.

3 METHODS

3.1 BACKGROUND

Let $s = (w_1, w_2, \dots, w_n)$ represent the input token sequence, where each w_i belongs to a fixed vocabulary. Let θ_{LLM} represent a Transformer-based large language model, which can calculate the conditional probability distribution of the next token $p(w_{n+1}|s; \theta_{\text{LLM}})$ and generate tokens iteratively. Typically, the input s is fixed. Therefore, the generation process of LLMs usually employs the KV Cache mechanism (Pope et al., 2023) to store previously computed Key/Value vectors during each layer’s attention calculation. We denote the KV cache as $\mathbf{K} = (K_1, K_2, \dots, K_n)$ and $\mathbf{V} = (V_1, V_2, \dots, V_n)$, where K_i and V_i are the keys and values associated with token w_i . When predicting the token at position $n + 1$, we can use w_n as input and, in each layer, compute the attention between the current hidden representation and the stored KV cache, avoiding recomputing the hidden representation of previous tokens. Without any confusion, we also denote the next token probability distribution as $p(w_{n+1}|\mathbf{K}, \mathbf{V}, w_n; \theta_{\text{LLM}})$.

In this study, we aim to investigate a new scenario where the context s is real-time edited by users, which makes it impossible for the KV cache to predict the correct next token without any modification. We can model such real-time context as a sequence of steps. Each step can be formulated as an action where tokens from position i to j in s are edited, resulting in a modified sequence $s^{\text{edit}} = [w_1, \dots, w_i, a_1, a_2, \dots, a_m, w_{j+1}, \dots, w_n]$, where $[a_1, a_2, \dots, a_m]$ represent the new inputs that replace $[w_i, \dots, w_j]$. Our goal is to accurately and efficiently predict w_{n+1} given by θ_{LLM} on s^{edit} . This problem is crucial in various scenarios. For instance, users can frequently edit their previous codes for different purposes and expect the code language model to swiftly adapt to these changes and predict the correct next line based on the updated information.

As the context between position i and position j is edited, the KV cache corresponding to these tokens must be updated. Furthermore, these changes will impact the representations of subsequent tokens after position j , thereby necessitating updates to all subsequent KV cache. The naive approach involves a full-recomputation strategy: re-encoding all the KV cache for $[a_1, a_2, \dots, a_m, w_{j+1}, \dots, w_n]$ layer by layer, followed by making predictions using the updated cache \mathbf{K}^* and \mathbf{V}^* . This approach ensures the KV cache is exact when predicting the next tokens. However, it is easy to see that it is computationally expensive, especially when the edits are light but the texts to be re-encoded are long. It’s worth noting that the original \mathbf{K} and \mathbf{V} already encode rich information on $[w_{j+1}, \dots, w_n]$, and a full recomputation may not be essential for practical problems. With this in mind, we seek to find ways to efficiently edit \mathbf{K} and \mathbf{V} , yielding \mathbf{K}^{edit} and \mathbf{V}^{edit} , which approximates $p(w_{n+1}|\mathbf{K}^*, \mathbf{V}^*, w_n; \theta_{\text{LLM}}) \approx p(w_{n+1}|\mathbf{K}^{\text{edit}}, \mathbf{V}^{\text{edit}}, w_n; \theta_{\text{LLM}})$ in an effective way.

3.2 POSITIONAL INTEGRITY ENCODING (PIE)

When a user modifies s into s^{edit} , KV cache associated with the first i tokens, i.e., $\mathbf{K}_{[1:i]}$ and $\mathbf{V}_{[1:i]}$, remains unchanged. As $[a_1, a_2, \dots, a_m]$ is the user’s new input, we feed this subsequence to the LLM to obtain the keys and values from position $i + 1$ to $i + m$. We denote this piece of new KV cache as $\mathbf{K}_{[i+1:i+m]}^{\text{edit}}$ and $\mathbf{V}_{[i+1:i+m]}^{\text{edit}}$, and now have the edited KV cache as:

$$\mathbf{K}^{\text{edit}} = \text{Concat}(\mathbf{K}_{[1:i]}, \mathbf{K}_{[i+1:i+m]}^{\text{edit}}, \mathbf{K}_{[j+1:n]}), \quad (1)$$

$$\mathbf{V}^{\text{edit}} = \text{Concat}(\mathbf{V}_{[1:i]}, \mathbf{V}_{[i+1:i+m]}^{\text{edit}}, \mathbf{V}_{[j+1:n]}), \quad (2)$$

where the red symbols indicate real-time calculations.

Challenges. The key challenge lies in how to edit the succeeding KV cache $\mathbf{K}_{[j+1:n]}$ and $\mathbf{V}_{[j+1:n]}$. Clearly, the modification of $[a_1, a_2, \dots, a_m]$ impacts the subsequent content in two ways: semantically and structurally. The semantic impact refers to the changes in the understanding of the subsequent text caused by the edited content. This can be a problem in natural language applications, such as dialog systems, where modifications to earlier conversations can significantly influence the generation of current responses. The other impact is structural, primarily concerning the temporal confusion between the pre-edit and post-edit sequences when $j - i \neq m$. This issue arises with common editing actions in code, such as additions and deletions (corresponding to $j - i = 0$ or $m = 0$). To be more concrete, imagine the original sequence has 5 tokens. If we add three tokens

between the second and third position, it will occupy the positional index [3, 4, 5]. We calculate $\mathbf{K}_{[3:5]}^{\text{edit}}$ and $\mathbf{V}_{[3:5]}^{\text{edit}}$ in equation (1) and (2). However, in the original $\mathbf{K}_{[3:5]}$ and $\mathbf{V}_{[3:5]}$, the positional index [3, 4, 5] is also occupied. If we integrate them together and take no actions during the next token prediction, the model will calculate similarity with multiple keys in the KV cache with the same index [3, 4, 5], causing confusion and potential prediction errors. Empirically, in code tasks, we find that the semantic impact is relatively small. Addressing temporal confusion for light edits alone can already lead to good performance (see the experiments in Section 4 for more details).

Our approach. To mitigate the temporal confusion during real-time editing, we propose a simple yet effective solution: **Positional Integrity Encoding (PIE)**, which ensures that positional information remains correctly ordered after editing without the need to re-encode the KV cache for subsequent tokens. PIE builds upon the rotary positional encoding (RoPE) (Su et al., 2021), which is the most widely used positional encoding in LLMs. Without loss of generality, given a query vector \mathbf{x}_i at position i and a key vector \mathbf{x}_j at position j , RoPE calculates the dot-product similarity using

$$z_{ij} = \mathbf{x}_i^T W_q^T \mathbf{R}_{j-i} W_k \mathbf{x}_j \quad (3)$$

where \mathbf{R}_{j-i} is the rotary matrix parameterized by the relative distance $j - i$, and W_q and W_k are learnable projection matrices. By definition, \mathbf{R}_{j-i} can be expressed by the multiplication of two rotary matrices:

$$\mathbf{R}_{j-i} = \mathbf{R}_i^T \mathbf{R}_j \quad (4)$$

For practical implementation, during inference, we compute $\mathbf{R}_{\Theta, i} W_k x_i$ as the key on the fly and store it in the cache, and when a query arrives at a new position, we rotate the query using its corresponding rotary matrix and calculate its similarity with all the keys in the cache to obtain the attention scores.

It can be easily seen that the positional information in the KV cache is encoded within the rotary matrix. When an edit occurs, the rotary matrix associated with the keys must be adjusted to reflect their post-edit locations. Leveraging the formulation of RoPE-based attention calculation, this challenge can be addressed by first removing the rotary matrices in \mathbf{K} that introduce temporal confusion and then reapplying the correct rotary matrix. In detail, assume we would like to update the key vector $\mathbf{k}_{j'}^l$ for the original position $j' \in [j + 1, n]$, where $l \in [1, L]$ is the layer index. We can simply edit the key vector by using

$$\mathbf{k}_{j'}^{\text{edit}, l} = \mathbf{R}_{i+m+j'-j} \mathbf{R}_{j'}^{-1} \mathbf{k}_{j'}^l \quad (5)$$

where $\mathbf{R}_{j'}^{-1}$, the inverse rotary matrix at position j' , is used to remove the incorrect positional information, and $\mathbf{R}_{i+m+j'-j}$ is used to encode the correct position $i + m + j' - j$ in s^{edit} . It can be easily seen that the computation can be further simplified as

$$\mathbf{k}_{j'}^{\text{edit}, l} = \mathbf{R}_{i+m+j'-j} \mathbf{R}_{j'}^{-1} \mathbf{k}_{j'}^l = \mathbf{R}_{i+m+j'-j} \mathbf{R}_{-j'} \mathbf{k}_{j'}^l = \mathbf{R}_{i+m-j} \mathbf{k}_{j'}^l \quad (6)$$

Hence, the full editing process for $\mathbf{K}_{[j+1:n]}$ is as follows:

$$\mathbf{K}_{[j+1:n]}^{\text{edit}} = [\mathbf{K}_{j+1}^{\text{edit}}, \dots, \mathbf{K}_n^{\text{edit}}] \quad (7)$$

$$\text{where each } \mathbf{K}_{j'}^{\text{edit}} = \{\mathbf{k}_{j'}^{\text{edit}, 1}, \dots, \mathbf{k}_{j'}^{\text{edit}, l}, \dots, \mathbf{k}_{j'}^{\text{edit}, L}\}, j' \in [j + 1, n], l \in [1, L]$$

$$\text{each } \mathbf{k}_{j'}^{\text{edit}, l} = \mathbf{R}_{i+m-j} \mathbf{k}_{j'}^l$$

Unlike the full recomputation approach, the above calculation only requires a single round of matrix multiplication to directly modify the pre-computed KV cache, where the computational overhead can be considered negligible. By utilizing these transformations, we finally construct the edited KV cache as:

$$\mathbf{K}^{\text{edit}} = \text{Concat}(\mathbf{K}_{[1:i]}, \mathbf{K}_{[i+1:i+m]}^{\text{edit}}, \mathbf{K}_{[j+1:n]}^{\text{edit}}), \quad (8)$$

$$\mathbf{V}^{\text{edit}} = \text{Concat}(\mathbf{V}_{[1:i]}, \mathbf{V}_{[i+1:i+m]}^{\text{edit}}, \mathbf{V}_{[j+1:n]}), \quad (9)$$

where the red symbols indicate real-time calculations. The LLM then makes predictions based on $p(x_{n+1} | \mathbf{K}^{\text{edit}}, \mathbf{V}^{\text{edit}}, x_n; \theta_{\text{LLM}})$. It is worth noting that PIE is compatible with KV cache eviction methods (Xiao et al., 2024; Zhang et al., 2024; Liu et al., 2024b). These KV cache eviction methods focus on reducing the memory usage of the KV cache during inference. PIE is designed to obtain the KV cache of the edited context with minimal overhead. By integrating PIE with KV cache eviction methods, it is possible to maintain efficient memory management while ensuring the integrity of the positional information in the real-time edit setting.

Table 1: Statistics of RepoBench-C-8k (Liu et al., 2024a) test set.

Language	XF-F	XF-R	IF	Average Number of Tokens
Python	18,000	7,500	10,500	3,967
Java	18,000	7,500	10,500	4,179

4 EXPERIMENTS

In this section, we empirically study the effectiveness of our proposed method. In particular, we aim at answering the following questions through experiments:

- **Question 1:** Can our Positional Integrity Encoding maintain the prediction accuracy of full re-computation in code editing scenarios?
- **Question 2:** How much efficiency improvement can be achieved by using our Positional Integrity Encoding compared to existing approaches?
- **Question 3:** How large is the gap between our Positional Integrity Encoding and full re-computation in terms of LLM’s predictions & representations?

We will answer each question with carefully designed experiments in the following sub-sections.

4.1 EXPERIMENTAL SETUP

Tasks. Our experiments are conducted on RepoBench-C-8k (Liu et al., 2024a). This benchmark focuses on the prediction of the next line of code, given a set of in-file context (including import statements and preceding lines before the target line), and cross-file context (comprising snippets from other files parsed by import statements). The detailed statistics of RepoBench-C-8k is shown in Table 1. To effectively evaluate next-line prediction performance of code LLMs, we follow Liu et al. (2024a) to use three task settings: (1) Cross-File-First (XF-F): mask the first appearance of a cross-file line within a file; (2) Cross-File-Random (XF-R): mask a random and non-first occurrence of a cross-file line; (3) In-File (IF): mask an in-file line that does not involve any cross-file modules. Moreover, we carefully design three real-world scenarios covering code insertion, code deletion, and code edition to comprehensively examine our approach. See Appendix A.1 for more detailed descriptions of tasks construction.

Settings. In our experiments, we employ DeepSeek-Coder (Guo et al., 2024), a code LLM that achieves strong performance in handling repository-level code completion tasks (We also conduct experiments on CodeLlama (Roziere et al., 2023) in Appendix A.2). We use Transformers (Wolf et al., 2020) as our codebase. We benchmark our method on models of different sizes covering 1.3B, 6.7B, and 33B. During inference, the greedy decoding strategy is used to deterministically generate 64 tokens. For 1.3B and 6.7B models, all the experiments are conducted on a single NVIDIA A100 GPU. For 33B models, the time for encoding the context is conducted on two NVIDIA A100 GPUs and the full generation process is conducted on eight NVIDIA A100 GPUs. The first non-comment line in the output is truncated and used as the prediction. The batch size is set to 1. All experiments are repeated three times with different seeds and the averaged scores are reported.

Evaluation. For comparison with our Positional Integrity Encoding, we choose two standard approaches as baselines: (1) Full-recomputation: re-compute the KV cache for all edited tokens and subsequent tokens; (2) Conflict Fast Encoding: re-compute the KV cache for the edited tokens while keeping the rest of the cache intact (i.e., using equation (1,2)). Following Lu et al. (2021), we use Exact Match (EM) and Edit Similarity (ES) (Svyatkovskiy et al., 2020) to evaluate the accuracy of the predicted code lines on code completion tasks. We also report the time required to encode the edited context for efficiency evaluation.

4.2 MAIN RESULTS

Positional Integrity Encoding perfectly preserves the full re-computation performance. Results of different code editing settings are presented in Table 2, 3 and 4 respectively. It can be easily seen

Table 2: **Performance comparisons of insertion experiments.** In this task, for each next-line prediction target, we insert several lines of code into its context randomly to simulate real-world scenarios. EM and ES denote the Exact Match and Edit Similarity score respectively. All results demonstrate that our Positional Integrity Encoding approach brings substantial speed-ups without performance drops.

	Model	Method	XF-F			XF-R			IF		
			EM	ES	Time	EM	ES	Time	EM	ES	Time
Python	1.3B	Full-recomputation	22.42	65.26	192ms	35.41	72.96	193ms	28.78	69.22	193ms
	1.3B	Conflict Fast Encoding	7.32	43.73	23ms	10.61	47.18	22ms	8.91	45.25	22ms
	1.3B	PIE	22.3	65.2	29ms	35.33	72.88	28ms	28.69	69.13	29ms
Python	6.7B	Full-recomputation	28.95	70.11	561ms	40.89	76.19	564ms	35.26	72.73	562ms
	6.7B	Conflict Fast Encoding	5.35	33.32	34ms	6.52	35.25	34ms	6.09	38.76	34ms
	6.7B	PIE	28.83	70.01	50ms	40.77	76.14	50ms	35.2	72.72	50ms
Python	33B	Full-recomputation	35.75	73.46	2194ms	46.0	78.9	2199ms	39.75	75.12	2194ms
	33B	Conflict Fast Encoding	3.96	30.13	126ms	5.41	32.32	121ms	3.92	35.56	127ms
	33B	PIE	35.77	73.45	134ms	45.74	78.85	140ms	39.74	75.1	141ms
Java	1.3B	Full-recomputation	26.21	70.89	200ms	36.77	76.31	200ms	45.89	78.04	198ms
	1.3B	Conflict Fast Encoding	0.29	3.12	22ms	0.57	3.19	23ms	0.7	2.63	23ms
	1.3B	PIE	26.13	70.82	30ms	36.67	76.25	30ms	45.92	77.99	29ms
Java	6.7B	Full-recomputation	32.51	75.56	578ms	41.97	79.41	578ms	50.86	80.53	578ms
	6.7B	Conflict Fast Encoding	0.47	2.77	34ms	0.76	2.78	35ms	0.67	2.48	33ms
	6.7B	PIE	32.21	75.47	50ms	41.96	79.32	49ms	50.85	80.43	48ms
Java	33B	Full-recomputation	35.05	76.93	2269ms	44.95	80.87	2281ms	53.23	81.76	2270ms
	33B	Conflict Fast Encoding	0.38	2.51	120ms	0.59	2.40	122ms	0.68	2.09	122ms
	33B	PIE	34.78	76.78	138ms	45.01	80.95	133ms	53.16	81.66	139ms

Table 3: **Performance comparisons of deletion experiments.** In this task, for each next-line prediction target, we delete several lines of code of its context randomly to simulate real-world scenarios. EM and ES denotes the Exact Match and Edit Similarity score respectively. All results demonstrate that our Positional Integrity Encoding approach brings substantial speed-ups without performance drops.

	Model	Method	XF-F			XF-R			IF		
			EM	ES	Time	EM	ES	Time	EM	ES	Time
Python	1.3B	Full-recomputation	22.42	65.26	192ms	35.41	72.96	193ms	28.78	69.22	193ms
	1.3B	Conflict Fast Encoding	0.41	39.31	22ms	0.59	42.02	24ms	1.05	42.85	22ms
	1.3B	PIE	22.31	65.19	29ms	35.25	72.81	27ms	28.8	69.16	27ms
Python	6.7B	Full-recomputation	28.95	70.11	561ms	40.89	76.19	564ms	35.26	72.73	562ms
	6.7B	Conflict Fast Encoding	0.51	40.24	30ms	0.77	42.77	31ms	1.42	43.93	30ms
	6.7B	PIE	28.86	70.01	43ms	40.77	76.15	42ms	35.09	72.67	42ms
Python	33B	Full-recomputation	35.75	73.46	2194ms	46.0	78.9	2199ms	39.75	75.12	2194ms
	33B	Conflict Fast Encoding	1.42	43.93	105ms	1.55	44.22	108ms	2.4	45.04	108ms
	33B	PIE	35.09	72.67	128ms	45.21	78.18	118ms	39.69	75.05	119ms
Java	1.3B	Full-recomputation	26.21	70.89	200ms	36.77	76.31	200ms	45.89	78.04	198ms
	1.3B	Conflict Fast Encoding	0.33	33.48	22ms	0.55	36.24	22ms	1.35	38.65	22ms
	1.3B	PIE	26.05	70.77	28ms	36.83	76.34	27ms	45.74	77.91	27ms
Java	6.7B	Full-recomputation	32.51	75.56	578ms	41.97	79.41	578ms	50.86	80.53	578ms
	6.7B	Conflict Fast Encoding	0.49	33.6	29ms	0.8	36.17	29ms	1.84	38.82	29ms
	6.7B	PIE	32.57	75.56	42ms	41.83	79.39	43ms	50.88	80.52	42ms
Java	33B	Full-recomputation	35.05	76.93	2269ms	44.95	80.87	2281ms	53.23	81.76	2270ms
	33B	Conflict Fast Encoding	0.91	35.06	109ms	1.01	37.97	106ms	2.31	40.15	105ms
	33B	PIE	34.82	76.76	117ms	44.93	80.86	120ms	53.19	81.71	119ms

that all metrics indicate that our Positional Integrity Encoding can perfectly maintain the prediction accuracy of full re-computation in different scenarios. This indicates that PIE effectively addresses temporal confusion, and the semantic impact of minor edits is relatively negligible. For example, in the most challenging XF-F setting requiring to handle long-range cross-file context, the maximum relative difference between our PIE and Full-recomputation across different model sizes and code languages is 0.3%/0.15%, 0.66%/0.79%, 1.33%/2.24% for code insertion, deletion, and edition in

Table 4: **Performance comparisons of edition experiments.** In this task, for each next-line prediction target, we delete several lines of code of its context and simultaneously insert other lines of code randomly to simulate real-world scenarios. EM and ES denote the Exact Match and Edit Similarity score respectively. All results demonstrate that our Positional Integrity Encoding approach brings substantial speed-ups without performance drops.

	Model	Method	XF-F			XF-R			IF		
			EM	ES	Time	EM	ES	Time	EM	ES	Time
Python	1.3B	Full-recomputation	22.42	65.26	242ms	35.41	72.96	242ms	28.78	69.22	244ms
	1.3B	Conflict Fast Encoding	8.80	50.08	23ms	13.83	54.01	22ms	11.29	51.99	22ms
	1.3B	PIE	22.04	64.59	30ms	34.49	72.02	29ms	28.15	68.32	29ms
Python	6.7B	Full-recomputation	28.95	70.11	705ms	40.89	76.19	706ms	35.26	72.73	713ms
	6.7B	Conflict Fast Encoding	11.26	51.63	34ms	12.57	53.27	34ms	12.75	51.45	34ms
	6.7B	PIE	28.07	69.00	54ms	39.89	75.10	54ms	34.05	71.64	54ms
Python	33B	Full-recomputation	35.75	73.46	2766ms	46.00	78.90	2759ms	39.75	75.12	2787ms
	33B	Conflict Fast Encoding	14.33	53.73	126ms	15.12	54.59	121ms	13.88	51.94	127ms
	33B	PIE	34.62	72.47	146ms	44.59	77.69	142ms	38.83	74.08	141ms
Java	1.3B	Full-recomputation	26.21	70.89	251ms	36.77	76.31	253ms	45.89	78.04	249ms
	1.3B	Conflict Fast Encoding	5.87	31.46	22ms	8.01	32.74	23ms	10.20	34.34	23ms
	1.3B	PIE	25.29	68.93	30ms	35.59	74.17	30ms	44.51	76.06	29ms
Java	6.7B	Full-recomputation	32.51	75.56	733ms	41.97	79.41	736ms	50.86	80.53	728ms
	6.7B	Conflict Fast Encoding	9.28	39.32	34ms	11.47	39.11	35ms	15.51	41.92	33ms
	6.7B	PIE	31.32	73.83	52ms	40.89	77.65	53ms	49.44	78.80	53ms
Java	33B	Full-recomputation	35.05	76.93	2892ms	44.95	80.87	2894ms	53.23	81.76	2833ms
	33B	Conflict Fast Encoding	8.02	32.93	120ms	9.67	33.29	122ms	12.10	34.70	122ms
	33B	PIE	33.72	74.69	134ms	43.71	78.66	138ms	51.71	79.49	143ms

terms of EM/ES respectively, which is rather negligible. This thorough examination serves as a strong support of the reliability of our PIE approach in real-world code editing scenarios.

Positional Integrity Encoding significantly reduces computational overhead. Moreover, we further benchmark the computational costs brought by different approaches. From all results in the above tables, it can be easily seen that our Positional Integrity Encoding can achieve substantial speed-up compared to full re-computation while preserving its performance simultaneously. In particular, for the code edition experiment that requires both insertion and deletion, the averaged reductions of computational overhead induced by our PIE are 87.9%/88.2%, 92.4%/92.8%, 94.8%/95.2% for 1.3B, 6.7B, and 33B models on Python/Java languages respectively. Furthermore, compared to Conflict Fast Encoding which induces minimal costs but largely hurts performance, our PIE only brings negligible overhead, showing its good accuracy-efficiency balance.

In summary, our main results comprehensively demonstrate the superiority of our Positional Integrity Encoding for code LLMs towards real-world code editing scenarios, which perfectly preserves the prediction accuracy and significantly addresses the crucial gap in the efficient deployment of LLMs in real-time dynamic scenarios.

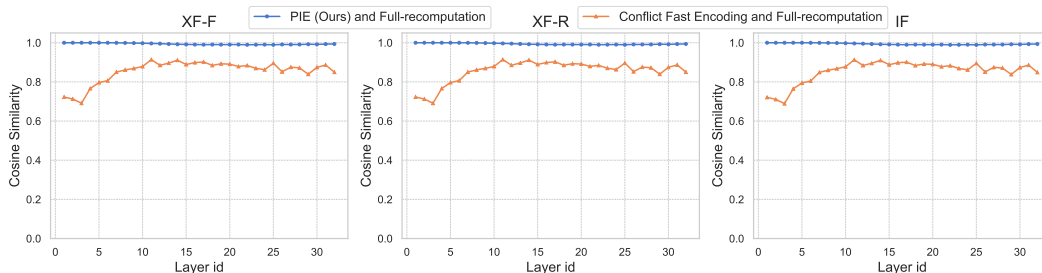
4.3 MORE ANALYSIS

In this subsection, we further present detailed analysis to investigate how large is the gap between our Positional Integrity Encoding and full re-computation in terms of context representations and predictions from LLMs, which provide additional insight of our approach.

How large is the gap on context representations? In practical scenarios, real-time editing by users results in the modified sequence \mathbf{x}^{edit} , requiring the KV cache to must be updated. In our analysis, we use the cosine similarity between context representations of full re-computation $\mathbf{K}_{[j+1:n]}^*$ and (1) our Positional Integrity Encoding $\mathbf{K}_{[j+1:n]}^{\text{edit}}$; (2) Conflict Fast Encoding $\mathbf{K}_{[j+1:n]}$. We employ the DeepSeek-Coder 6.7B model on the Python subset of RepoBench. Averaged results are reported.

In Figure 3, the cosine similarity between representations of full re-computation and our Positional Integrity Encoding is consistently around 1.0 across all layers. This high similarity demonstrates the

432
433
434
435
436
437
438
439
440
441



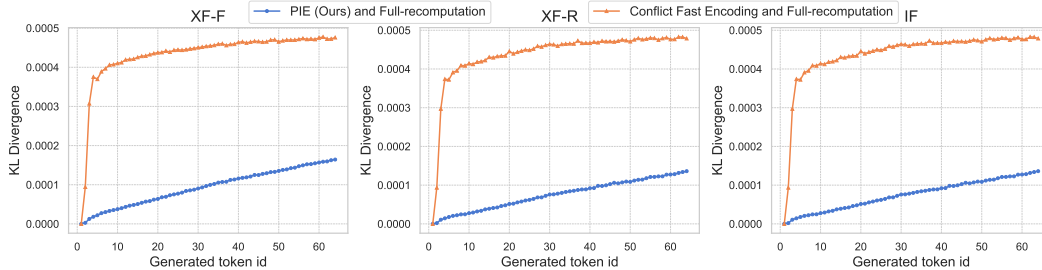
442 Figure 3: Cosine similarity of key representations across model layers. The plots compare the cosine
443 similarity between $K_{[j+1:n]}$ and $K_{[j+1:n]}^*$ (indicating temporal confusion of Conflict Fast Encoding)
444 with the cosine similarity between $K_{[j+1:n]}^{\text{edit}}$ and $K_{[j+1:n]}^*$ (showing the effectiveness of PIE).
445

446
447
448
449
450

effectiveness of PIE in preserving the contextual integrity of the key representations after editing,
suggesting that PIE successfully mitigates the temporal confusion that typically arises when manipu-
lating the KV cache. In contrast, the cosine similarity between representations of full re-computation
and Conflict Fast Encoding is significantly lower, indicating the temporal confusion issue that hurts
model performance a lot.

451

452
453
454
455
456
457
458
459
460



461 Figure 4: KL divergence of the generated token distributions. The plots compare the KL divergence
462 between the generated token distributions of PIE and Full-recomputation, and the KL divergence
463 between the generated token distributions of Conflict Fast Encoding and Full-recomputation.
464

465
466
467
468
469
470
471
472

How large is the gap on model predictions? Moreover, we further use Kullback-Leibler (KL)
divergence as the metric to investigate the gap between model predictions of different approaches.
Similarly, we employ the DeepSeek-Coder 6.7B model on the Python subset of RepoBench and report
the averaged results. In Figure 4, the KL divergence between model predictions of full re-computation
and our Positional Integrity Encoding remains consistently low, i.e., below 0.0002 across 64 tokens.
However, the KL divergence between model predictions of full re-computation and Conflict Fast
Encoding is substantially higher (2x larger). These findings again underscore the importance of
maintaining positional integrity within the KV cache to ensure accurate generation results.

473

474 **5 CONCLUSION**

475
476
477
478
479
480
481

In this paper, we introduce Positional Integrity Encoding (PIE), a novel method designed to enhance
the efficiency of large language models (LLMs) in the real-time editing setting. Our approach
addresses the significant computational overhead associated with re-encoding contexts after small
edits, a common scenario in interactive coding environments. Through extensive experiments,
we demonstrated that PIE not only significantly reduces latency but also maintains high accuracy
compared to the naive full re-computation method.

482
483
484
485

PIE represents a substantial step forward in the development of efficient LLMs, particularly in
dynamic contexts where frequent edits are made. Future work could explore the integration of
PIE with other optimization techniques and its application to a broader range of tasks beyond code
generation. Our method paves the way for more responsive and resource-efficient AI assistants,
enhancing their practicality and usability in various real-world scenarios.

REFERENCES

- 486
487
488 Amey Agrawal, Nitin Kedia, Ashish Panwar, Jayashree Mohan, Nipun Kwatra, Bhargav S Gulavani,
489 Alexey Tumanov, and Ramachandran Ramjee. Taming throughput-latency tradeoff in llm inference
490 with sarathi-serve. *arXiv preprint arXiv:2403.02310*, 2024.
- 491
492 Rohan Anil, Andrew M Dai, Orhan Firat, Melvin Johnson, Dmitry Lepikhin, Alexandre Passos,
493 Siamak Shakeri, Emanuel Taropa, Paige Bailey, Zhifeng Chen, et al. Palm 2 technical report. *arXiv*
494 *preprint arXiv:2305.10403*, 2023.
- 495
496 Iz Beltagy, Matthew E. Peters, and Arman Cohan. Longformer: The long-document transformer.
497 *arXiv:2004.05150*, 2020.
- 498
499 Tianle Cai, Yuhong Li, Zhengyang Geng, Hongwu Peng, Jason D Lee, Deming Chen, and Tri Dao.
500 Medusa: Simple llm inference acceleration framework with multiple decoding heads. *arXiv*
501 *preprint arXiv:2401.10774*, 2024.
- 502
503 Charlie Chen, Sebastian Borgeaud, Geoffrey Irving, Jean-Baptiste Lespiau, Laurent Sifre, and John
504 Jumper. Accelerating large language model decoding with speculative sampling. *arXiv preprint*
505 *arXiv:2302.01318*, 2023. URL <https://arxiv.org/abs/2302.01318>.
- 506
507 Ta-Chung Chi, Ting-Han Fan, Peter J Ramadge, and Alexander Rudnicky. Kerple: Kernelized
508 relative positional embedding for length extrapolation. *Advances in Neural Information Processing*
509 *Systems*, 35:8386–8399, 2022.
- 510
511 Ta-Chung Chi, Ting-Han Fan, Alexander Rudnicky, and Peter Ramadge. Dissecting transformer
512 length extrapolation via the lens of receptive field analysis. In *Proceedings of the 61st Annual*
513 *Meeting of the Association for Computational Linguistics (Volume 1: Long Papers)*, pp. 13522–
514 13537, 2023.
- 515
516 Rewon Child, Scott Gray, Alec Radford, and Ilya Sutskever. Generating long sequences with sparse
517 transformers. *arXiv preprint arXiv:1904.10509*, 2019.
- 518
519 Krzysztof Marcin Choromanski, Valerii Likhoshesterov, David Dohan, Xingyou Song, Andreea
520 Gane, Tamas Sarlos, Peter Hawkins, Jared Quincy Davis, Afroz Mohiuddin, Lukasz Kaiser, et al.
521 Rethinking attention with performers. In *International Conference on Learning Representations*,
522 2021.
- 523
524 Zihang Dai, Zhilin Yang, Yiming Yang, Jaime Carbonell, Quoc Le, and Ruslan Salakhutdinov.
525 Transformer-XL: Attentive language models beyond a fixed-length context. In *acl*, July 2019.
- 526
527 Tri Dao. Flashattention-2: Faster attention with better parallelism and work partitioning. *arXiv*
528 *preprint arXiv:2307.08691*, 2023. URL <https://arxiv.org/abs/2307.08691>.
- 529
530 Tri Dao, Dan Fu, Stefano Ermon, Atri Rudra, and Christopher Ré. Flashattention: Fast and memory-
531 efficient exact attention with io-awareness. In *Advances in Neural Information Processing Systems*
532 *(NeurIPS)*, 2022. URL https://proceedings.neurips.cc/paper_files/paper/2022/file/67d57c32e20fd0a7a302cb81d36e40d5-Paper-Conference.pdf.
- 533
534 Tim Dettmers, Mike Lewis, Younes Belkada, and Luke Zettlemoyer. Gpt3. int8 (): 8-bit matrix
535 multiplication for transformers at scale. In *Advances in Neural Information Processing Systems*
536 *(NeurIPS)*, 2022. URL <https://arxiv.org/abs/2208.07339>.
- 537
538 Elias Frantar and Dan Alistarh. Sparsegpt: Massive language models can be accurately pruned in
539 one-shot. In *International Conference on Machine Learning*, pp. 10323–10337. PMLR, 2023.
- 534
535 Elias Frantar, Saleh Ashkboos, Torsten Hoefler, and Dan Alistarh. Optq: Accurate quantization
536 for generative pre-trained transformers. In *The Eleventh International Conference on Learning*
537 *Representations*, 2022. URL https://openreview.net/forum?id=tcbBPnfwxS&fbclid=IwAR0QoRRF_7gr6NEt2sKchK5wgGNLfJUNavvbSeCR1WhpVmtUbo0W3ExJXZE.
- 538
539 Yao Fu. Challenges in deploying long-context transformers: A theoretical peak performance analysis.
arXiv preprint arXiv:2405.08944, 2024.

- 540 Yuxian Gu, Li Dong, Furu Wei, and Minlie Huang. Minillm: Knowledge distillation of large language
541 models. In *The Twelfth International Conference on Learning Representations*, 2024.
- 542
- 543 Daya Guo, Qihao Zhu, Dejian Yang, Zhenda Xie, Kai Dong, Wentao Zhang, Guanting Chen, Xiao
544 Bi, Y Wu, YK Li, et al. Deepseek-coder: When the large language model meets programming—the
545 rise of code intelligence. *arXiv preprint arXiv:2401.14196*, 2024.
- 546 Zhenyu He, Zexuan Zhong, Tianle Cai, Jason D Lee, and Di He. Rest: Retrieval-based speculative
547 decoding. *arXiv preprint arXiv:2311.08252*, 2023.
- 548
- 549 Zhenyu He, Guhao Feng, Shengjie Luo, Kai Yang, Di He, Jingjing Xu, Zhi Zhang, Hongxia Yang, and
550 Liwei Wang. Two stones hit one bird: Bilevel positional encoding for better length extrapolation.
551 *arXiv preprint arXiv:2401.16421*, 2024.
- 552 Itay Hubara, Brian Chmiel, Moshe Island, Ron Banner, Joseph Naor, and Daniel Soudry. Accelerated
553 sparse neural training: A provable and efficient method to find n : m transposable masks. In
554 *Advances in Neural Information Processing Systems (NeurIPS)*, 2021. URL [https://arxiv.org/
555 abs/2102.08124](https://arxiv.org/abs/2102.08124).
- 556 Angelos Katharopoulos, Apoorv Vyas, Nikolaos Pappas, and François Fleuret. Transformers are rns:
557 Fast autoregressive transformers with linear attention. In *International conference on machine
558 learning*, pp. 5156–5165. PMLR, 2020.
- 559
- 560 Nikita Kitaev, Łukasz Kaiser, and Anselm Levskaya. Reformer: The efficient transformer. *arXiv
561 preprint arXiv:2001.04451*, 2020.
- 562
- 563 Woosuk Kwon, Zhuohan Li, Siyuan Zhuang, Ying Sheng, Lianmin Zheng, Cody Hao Yu, Joseph
564 Gonzalez, Hao Zhang, and Ion Stoica. Efficient memory management for large language model
565 serving with pagedattention. In *Symposium on Operating Systems Principles (SOSP)*, 2023. URL
566 <https://arxiv.org/abs/2309.06180>.
- 567 Yaniv Leviathan, Matan Kalman, and Yossi Matias. Fast inference from transformers via speculative
568 decoding. In Andreas Krause, Emma Brunskill, Kyunghyun Cho, Barbara Engelhardt, Sivan
569 Sabato, and Jonathan Scarlett (eds.), *International Conference on Machine Learning (ICML)*, 2023.
570 URL <https://proceedings.mlr.press/v202/leviathan23a.html>.
- 571 Shanda Li, Chong You, Guru Guruganesh, Joshua Ainslie, Santiago Ontanon, Manzil Zaheer, Sumit
572 Sanghai, Yiming Yang, Sanjiv Kumar, and Srinadh Bhojanapalli. Functional interpolation for
573 relative positions improves long context transformers. *arXiv preprint arXiv:2310.04418*, 2023.
- 574
- 575 Yuhui Li, Fangyun Wei, Chao Zhang, and Hongyang Zhang. Eagle: Speculative sampling requires
576 rethinking feature uncertainty. In *International Conference on Machine Learning*, 2024.
- 577 Tianyang Liu, Canwen Xu, and Julian McAuley. Repobench: Benchmarking repository-level code
578 auto-completion systems, 2024a. URL <https://arxiv.org/abs/2306.03091>.
- 579
- 580 Ze Liu, Yutong Lin, Yue Cao, Han Hu, Yixuan Wei, Zheng Zhang, Stephen Lin, and Baining Guo.
581 Swin transformer: Hierarchical vision transformer using shifted windows. In *Proceedings of the
582 IEEE/CVF international conference on computer vision*, pp. 10012–10022, 2021.
- 583 Zechun Liu, Barlas Oguz, Changsheng Zhao, Ernie Chang, Pierre Stock, Yashar Mehdad, Yangyang
584 Shi, Raghuraman Krishnamoorthi, and Vikas Chandra. Llm-qat: Data-free quantization aware
585 training for large language models. *arXiv preprint arXiv:2305.17888*, 2023. URL [https://arxiv.
586 org/abs/2305.17888](https://arxiv.org/abs/2305.17888).
- 587
- 588 Zichang Liu, Aditya Desai, Fangshuo Liao, Weitao Wang, Victor Xie, Zhaozhuo Xu, Anastasios
589 Kyriillidis, and Anshumali Shrivastava. Scissorhands: Exploiting the persistence of importance
590 hypothesis for llm kv cache compression at test time. *Advances in Neural Information Processing
591 Systems*, 36, 2024b.
- 592 Shuai Lu, Daya Guo, Shuo Ren, Junjie Huang, Alexey Svyatkovskiy, Ambrosio Blanco, Colin
593 Clement, Dawn Drain, Daxin Jiang, Duyu Tang, et al. Codexglue: A machine learning benchmark
dataset for code understanding and generation. *arXiv preprint arXiv:2102.04664*, 2021.

- 594 Shengjie Luo, Shanda Li, Tianle Cai, Di He, Dinglan Peng, Shuxin Zheng, Guolin Ke, Liwei Wang,
595 and Tie-Yan Liu. Stable, fast and accurate: Kernelized attention with relative positional encoding.
596 *Advances in Neural Information Processing Systems*, 34:22795–22807, 2021.
597
- 598 Shengjie Luo, Shanda Li, Shuxin Zheng, Tie-Yan Liu, Liwei Wang, and Di He. Your transformer
599 may not be as powerful as you expect. *Advances in Neural Information Processing Systems*, 35:
600 4301–4315, 2022.
- 601 Shengjie Luo, Tianlang Chen, Yixian Xu, Shuxin Zheng, Tie-Yan Liu, Liwei Wang, and Di He. One
602 transformer can understand both 2d & 3d molecular data. In *The Eleventh International Conference*
603 *on Learning Representations*, 2023. URL <https://openreview.net/forum?id=vZTp1oPV3PC>.
604
- 605 Xinyin Ma, Gongfan Fang, and Xinchao Wang. Llm-pruner: On the structural pruning of large
606 language models. In *Advances in Neural Information Processing Systems (NeurIPS)*, 2023. URL
607 <https://arxiv.org/pdf/2305.11627.pdf>.
- 608 Xupeng Miao, Gabriele Oliaro, Zhihao Zhang, Xinhao Cheng, Zeyu Wang, Rae Ying Yee Wong,
609 Zhuoming Chen, Daiyaan Arfeen, Reyna Abhyankar, and Zhihao Jia. Specinfer: Accelerating
610 generative llm serving with speculative inference and token tree verification. *arXiv preprint*
611 *arXiv:2305.09781*, 2023. URL <https://arxiv.org/abs/2305.09781>.
612
- 613 Gunho Park, Baeseong Park, Se Jung Kwon, Byeongwook Kim, Youngjoo Lee, and Dongsoo Lee.
614 nuqmm: Quantized matmul for efficient inference of large-scale generative language models. *arXiv*
615 *preprint arXiv:2206.09557*, 2022. URL <https://arxiv.org/abs/2206.09557>.
- 616 Reiner Pope, Sholto Douglas, Aakanksha Chowdhery, Jacob Devlin, James Bradbury, Jonathan
617 Heek, Kefan Xiao, Shivani Agrawal, and Jeff Dean. Efficiently scaling transformer inference.
618 *Proceedings of Machine Learning and Systems*, 5:606–624, 2023.
619
- 620 Ofir Press, Noah Smith, and Mike Lewis. Train short, test long: Attention with linear biases enables
621 input length extrapolation. In *International Conference on Learning Representations (ICLR)*, 2022.
622
- 623 Jiezhong Qiu, Hao Ma, Omer Levy, Wen-tau Yih, Sinong Wang, and Jie Tang. Blockwise self-
624 attention for long document understanding. In *Findings of the Association for Computational*
625 *Linguistics: EMNLP 2020*, pp. 2555–2565, 2020.
- 626 Colin Raffel, Noam Shazeer, Adam Roberts, Katherine Lee, Sharan Narang, Michael Matena, Yanqi
627 Zhou, Wei Li, and Peter J Liu. Exploring the limits of transfer learning with a unified text-to-text
628 transformer. *The Journal of Machine Learning Research*, 21(1):5485–5551, 2020.
- 629 Aurko Roy, Mohammad Saffar, Ashish Vaswani, and David Grangier. Efficient content-based sparse
630 attention with routing transformers. *Transactions of the Association for Computational Linguistics*,
631 9:53–68, 2021.
632
- 633 Baptiste Roziere, Jonas Gehring, Fabian Gloeckle, Sten Sootla, Itai Gat, Xiaoqing Ellen Tan, Yossi
634 Adi, Jingyu Liu, Romain Sauvestre, Tal Remez, et al. Code llama: Open foundation models for
635 code. *arXiv preprint arXiv:2308.12950*, 2023.
- 636 Victor Sanh, Lysandre Debut, Julien Chaumond, and Thomas Wolf. Distilbert, a distilled version
637 of bert: smaller, faster, cheaper and lighter. *arXiv preprint arXiv:1910.01108*, 2019. URL
638 <https://arxiv.org/abs/1910.01108>.
639
- 640 Peter Shaw, Jakob Uszkoreit, and Ashish Vaswani. Self-attention with relative position representations.
641 In *Association for Computational Linguistics (ACL)*, June 2018.
- 642 Ying Sheng, Lianmin Zheng, Binhang Yuan, Zhuohan Li, Max Ryabinin, Beidi Chen, Percy Liang,
643 Christopher Ré, Ion Stoica, and Ce Zhang. Flexgen: High-throughput generative inference of
644 large language models with a single gpu. In *International Conference on Machine Learning*, pp.
645 31094–31116. PMLR, 2023.
646
- 647 Benjamin Spector and Chris Re. Accelerating llm inference with staged speculative decoding. *arXiv*
preprint arXiv:2308.04623, 2023. URL <https://arxiv.org/abs/2308.04623>.

- 648 Mitchell Stern, Noam Shazeer, and Jakob Uszkoreit. Blockwise parallel decoding for
649 deep autoregressive models. In *Advances in Neural Information Processing Systems*
650 (*NeurIPS*), 2018. URL [https://proceedings.neurips.cc/paper_files/paper/2018/file/
651 c4127b9194fe8562c64dc0f5bf2c93bc-Paper.pdf](https://proceedings.neurips.cc/paper_files/paper/2018/file/c4127b9194fe8562c64dc0f5bf2c93bc-Paper.pdf).
- 652 Jianlin Su, Yu Lu, Shengfeng Pan, Ahmed Murtadha, Bo Wen, and Yunfeng Liu. Roformer: Enhanced
653 transformer with rotary position embedding, 2021.
- 654 Yutao Sun, Li Dong, Barun Patra, Shuming Ma, Shaohan Huang, Alon Benhaim, Vishrav Chaudhary,
655 Xia Song, and Furu Wei. A length-extrapolatable transformer. In *Proceedings of the 61st Annual
656 Meeting of the Association for Computational Linguistics (Volume 1: Long Papers)*. Association
657 for Computational Linguistics, July 2023.
- 658 Alexey Svyatkovskiy, Shao Kun Deng, Shengyu Fu, and Neel Sundaresan. Intellicode compose:
659 Code generation using transformer. In *Proceedings of the 28th ACM joint meeting on European
660 software engineering conference and symposium on the foundations of software engineering*, pp.
661 1433–1443, 2020.
- 662 Yi Tay, Dara Bahri, Liu Yang, Donald Metzler, and Da-Cheng Juan. Sparse sinkhorn attention. In
663 *International Conference on Machine Learning*, pp. 9438–9447. PMLR, 2020.
- 664 Hugo Touvron, Louis Martin, Kevin Stone, Peter Albert, Amjad Almahairi, Yasmine Babaei, Nikolay
665 Bashlykov, Soumya Batra, Prajjwal Bhargava, Shruti Bhosale, et al. Llama 2: Open foundation
666 and fine-tuned chat models. *arXiv preprint arXiv:2307.09288*, 2023.
- 667 Ashish Vaswani, Noam Shazeer, Niki Parmar, Jakob Uszkoreit, Llion Jones, Aidan N Gomez, Łukasz
668 Kaiser, and Illia Polosukhin. Attention is all you need. *Advances in Neural Information Processing
669 Systems (NeurIPS)*, 30, 2017.
- 670 Hanrui Wang, Zhekai Zhang, and Song Han. Spatten: Efficient sparse attention architecture with
671 cascade token and head pruning. In *2021 IEEE International Symposium on High-Performance
672 Computer Architecture (HPCA)*, 2021. URL <https://arxiv.org/abs/2012.09852>.
- 673 Sinong Wang, Belinda Z Li, Madian Khabsa, Han Fang, and Hao Ma. Linformer: Self-attention with
674 linear complexity. *arXiv preprint arXiv:2006.04768*, 2020.
- 675 Thomas Wolf, Lysandre Debut, Victor Sanh, Julien Chaumond, Clement Delangue, Anthony Moi,
676 Pierric Cistac, Tim Rault, Rémi Louf, Morgan Funtowicz, Joe Davison, Sam Shleifer, Patrick
677 von Platen, Clara Ma, Yacine Jernite, Julien Plu, Canwen Xu, Teven Le Scao, Sylvain Gugger,
678 Mariama Drame, Quentin Lhoest, and Alexander M. Rush. Transformers: State-of-the-art natural
679 language processing. In *Proceedings of the 2020 Conference on Empirical Methods in Natural
680 Language Processing: System Demonstrations*, pp. 38–45, Online, October 2020. Association for
681 Computational Linguistics. URL [https://www.aclweb.org/anthology/2020.emnlp-demos.
682 6](https://www.aclweb.org/anthology/2020.emnlp-demos.6).
- 683 Guangxuan Xiao, Ji Lin, Mickael Seznec, Hao Wu, Julien Demouth, and Song Han. Smoothquant:
684 Accurate and efficient post-training quantization for large language models. In *International
685 Conference on Machine Learning (ICML)*, 2023. URL [https://proceedings.mlr.press/
686 v202/xiao23c/xiao23c.pdf](https://proceedings.mlr.press/v202/xiao23c/xiao23c.pdf).
- 687 Guangxuan Xiao, Yuandong Tian, Beidi Chen, Song Han, and Mike Lewis. Efficient streaming
688 language models with attention sinks. In *The Twelfth International Conference on Learning
689 Representations*, 2024. URL <https://openreview.net/forum?id=NG7sS51zVF>.
- 690 Zhewei Yao, Reza Yazdani Aminabadi, Minjia Zhang, Xiaoxia Wu, Conglong Li, and
691 Yuxiong He. Zeroquant: Efficient and affordable post-training quantization for
692 large-scale transformers. In *Advances in Neural Information Processing Systems*
693 (*NeurIPS*), 2022. URL [https://proceedings.neurips.cc/paper_files/paper/2022/file/
694 adf7fa39d65e2983d724ff7da57f00ac-Paper-Conference.pdf](https://proceedings.neurips.cc/paper_files/paper/2022/file/adf7fa39d65e2983d724ff7da57f00ac-Paper-Conference.pdf).
- 695 Chengxuan Ying, Tianle Cai, Shengjie Luo, Shuxin Zheng, Guolin Ke, Di He, Yanming Shen, and
696 Tie-Yan Liu. Do transformers really perform badly for graph representation? *Advances in neural
697 information processing systems*, 34:28877–28888, 2021.

702 Aohan Zeng, Xiao Liu, Zhengxiao Du, Zihan Wang, Hanyu Lai, Ming Ding, Zhuoyi Yang, Yifan
703 Xu, Wendi Zheng, Xiao Xia, Weng Lam Tam, Zixuan Ma, Yufei Xue, Jidong Zhai, Wenguang
704 Chen, Zhiyuan Liu, Peng Zhang, Yuxiao Dong, and Jie Tang. GLM-130b: An open bilingual
705 pre-trained model. In *The Eleventh International Conference on Learning Representations*, 2023.
706 URL <https://openreview.net/forum?id=-Aw0rrrPUF>.

707 Bohang Zhang, Shengjie Luo, Liwei Wang, and Di He. Rethinking the expressive power of GNNs
708 via graph biconnectivity. In *The Eleventh International Conference on Learning Representations*,
709 2023a. URL <https://openreview.net/forum?id=r9hNv76KoT3>.

710 Jun Zhang, Jue Wang, Huan Li, Lidan Shou, Ke Chen, Gang Chen, and Sharad Mehrotra. Draft &
711 verify: Lossless large language model acceleration via self-speculative decoding. *arXiv preprint*
712 *arXiv:2309.08168*, 2023b.

713 Zhenyu Zhang, Ying Sheng, Tianyi Zhou, Tianlong Chen, Lianmin Zheng, Ruisi Cai, Zhao Song,
714 Yuandong Tian, Christopher Ré, Clark Barrett, et al. H2o: Heavy-hitter oracle for efficient
715 generative inference of large language models. *Advances in Neural Information Processing*
716 *Systems*, 36, 2024.
717

718 A EXPERIMENTAL DETAILS

719 A.1 EXPERIMENTAL SETUP

720
721 **Tasks Construction for Code Insertion.** To simulate code insertion tasks, we start by randomly
722 deleting five consecutive lines from each context. The resulting context, which lacks these five lines,
723 is considered the original context. The complete context, which includes the previously deleted lines,
724 is treated as the edited context. The tokens within the deleted lines are identified as the inserted
725 tokens (around 64 tokens for Python and 51 tokens for Java). This setup allows us to evaluate the
726 model’s capability to accurately restore missing code segments, mimicking real-world scenarios
727 where developers frequently insert blocks of code.
728

729
730 **Tasks Construction for Code Deletion.** For code deletion tasks, we begin by randomly selecting a
731 line within the context and then inserting five randomly sampled lines at this position. The context
732 containing these additional lines is designated as the original context. The complete context, which
733 excludes the inserted lines, is regarded as the edited context. The tokens in the inserted lines are
734 treated as the deleted tokens (around 64 tokens for Python and 51 tokens for Java). This construction
735 enables us to assess the model’s performance in identifying and removing extraneous code, reflecting
736 situations where developers need to clean up or refactor their codebase.
737

738 **Tasks Construction for Multi-place Code Edition** To comprehensively evaluate the model’s
739 performance in handling simultaneous code insertion and deletion, we construct a task scenario that
740 integrates both operations. Initially, we randomly delete five consecutive lines from each context to
741 simulate code insertion. The context without these lines is treated as the original context. The tokens
742 in the deleted lines are identified as the inserted tokens.

743 Simultaneously, we randomly select another line within the context and insert five randomly sampled
744 lines at this position. The complete context, which includes all lines as they appear after both
745 deletions and insertions, is regarded as the edited context. The tokens in the newly inserted lines are
746 considered the deleted tokens. This dual operation setup allows us to evaluate the model’s ability to
747 handle complex, simultaneous edits, adding missing code segments while removing extraneous ones,
748 reflecting the multifaceted nature of real-world coding environments where developers often perform
749 multiple types of edits concurrently.

750 A.2 RESULTS ON CODELLAMA

751
752 Results of different code editing settings on CodeLlama (Roziere et al., 2023) are presented in
753 Table 5, 6 and 7 respectively. Similar to DeepSeek-Coder, CodeLlama with Positional Integrity
754 Encoding demonstrates strong performance and fast speed across various editing scenarios. The
755 metrics indicate that PIE effectively maintains prediction accuracy and addresses temporal confusion,
ensuring the impact of minor edits is minimal.

Table 5: **Performance comparisons of insertion experiments for CodeLlama.** In this task, for each next-line prediction target, we insert several lines of code into its context randomly to simulate real-world scenarios. EM and ES denotes the Exact Match and Edit Similarity score respectively. All results demonstrate that our Positional Integrity Encoding approach brings substantial speed-ups without performance drops.

	Model	Method	XF-F			XF-R			IF		
			EM	ES	Time	EM	ES	Time	EM	ES	Time
Python	7B	Full-recomputation	25.72	66.49	561ms	38.87	73.81	564ms	33.55	70.26	562ms
	7B	Conflict Fast Encoding	14.49	55.10	34ms	19.32	57.34	34ms	15.49	53.05	34ms
	7B	PIE	25.42	66.40	50ms	38.76	73.83	50ms	33.30	70.11	50ms
Python	34B	Full-recomputation	31.04	69.48	2013ms	42.80	76.27	2029ms	37.69	72.36	1999ms
	34B	Conflict Fast Encoding	11.56	50.23	113ms	16.06	52.59	110ms	11.58	48.36	112ms
	34B	PIE	30.53	68.79	123ms	42.73	76.40	119ms	37.51	72.25	123ms
Java	7B	Full-recomputation	28.02	72.49	578ms	39.61	77.81	578ms	49.20	79.76	578ms
	7B	Conflict Fast Encoding	10.45	37.69	34ms	14.28	38.45	35ms	16.95	38.15	33ms
	7B	PIE	28.02	72.39	50ms	39.48	77.74	49ms	49.31	79.79	48ms
Java	34B	Full-recomputation	32.16	75.09	2179ms	43.45	79.89	2184ms	52.43	80.97	2197ms
	34B	Conflict Fast Encoding	12.04	41.76	104ms	14.25	39.19	107ms	17.29	38.50	109ms
	34B	PIE	31.45	74.64	119ms	43.54	79.80	118ms	52.42	81.00	115ms

Table 6: **Performance comparisons of deletion experiments for CodeLlama.** In this task, for each next-line prediction target, we delete several lines of code of its context randomly to simulate real-world scenarios. EM and ES denote the Exact Match and Edit Similarity score respectively. All results demonstrate that our Positional Integrity Encoding approach brings substantial speed-ups without performance drops.

	Model	Method	XF-F			XF-R			IF		
			EM	ES	Time	EM	ES	Time	EM	ES	Time
Python	7B	Full-recomputation	25.72	66.49	561ms	38.87	73.81	564ms	33.55	70.26	562ms
	7B	Conflict Fast Encoding	10.14	52.80	30ms	15.24	57.88	31ms	13.04	54.53	30ms
	7B	PIE	25.52	66.47	43ms	38.88	73.87	42ms	33.51	70.18	42ms
Python	34B	Full-recomputation	31.04	69.48	2013ms	42.80	76.27	2029ms	37.69	72.36	1999ms
	34B	Conflict Fast Encoding	12.15	54.76	88ms	16.40	59.29	94ms	13.78	55.90	93ms
	34B	PIE	31.01	69.44	100ms	42.76	76.13	100ms	37.60	72.38	102ms
Java	7B	Full-recomputation	28.02	72.49	578ms	39.61	77.81	578ms	49.20	79.76	578ms
	7B	Conflict Fast Encoding	7.21	42.51	29ms	7.77	43.86	29ms	8.78	44.46	29ms
	7B	PIE	28.01	72.45	42ms	39.51	77.78	42ms	49.30	79.80	42ms
Java	34B	Full-recomputation	32.16	75.09	2179ms	43.45	79.89	2184ms	52.43	80.97	2197ms
	34B	Conflict Fast Encoding	8.76	45.44	92ms	8.67	45.57	92ms	10.11	46.64	95ms
	34B	PIE	32.12	75.02	99ms	43.33	79.86	98ms	52.36	80.96	107ms

Table 7: **Performance comparisons of edition experiments for CodeLlama.** In this task, for each next-line prediction target, we delete several lines of code of its context and simultaneously insert other lines of code randomly to simulate real-world scenarios. EM and ES denote the Exact Match and Edit Similarity score respectively. All results demonstrate that our Positional Integrity Encoding approach brings substantial speed-ups without performance drops.

	Model	Method	XF-F			XF-R			IF		
			EM	ES	Time	EM	ES	Time	EM	ES	Time
Python	7B	Full-recomputation	25.72	66.49	705ms	38.87	73.81	706ms	33.55	70.26	713ms
	7B	Conflict Fast Encoding	19.97	61.46	34ms	29.79	67.31	34ms	24.70	63.28	34ms
	7B	PIE	24.97	66.04	54ms	38.21	73.40	54ms	32.84	69.66	54ms
Python	34B	Full-recomputation	31.04	69.48	2574ms	42.80	76.27	2569ms	37.69	72.36	2581ms
	34B	Conflict Fast Encoding	21.91	61.78	91ms	30.87	67.16	91ms	25.76	63.15	90ms
	34B	PIE	29.92	68.7	126ms	41.74	75.37	126ms	37.01	71.76	127ms
Java	7B	Full-recomputation	28.02	72.49	733ms	39.61	77.81	736ms	49.20	79.76	728ms
	7B	Conflict Fast Encoding	18.78	57.38	34ms	25.79	60.97	35ms	32.60	62.66	33ms
	7B	PIE	27.43	71.60	52ms	38.89	76.96	53ms	48.60	78.94	53ms
Java	34B	Full-recomputation	32.16	75.09	2726ms	43.45	79.89	2807ms	52.43	80.97	2727ms
	34B	Conflict Fast Encoding	21.25	59.70	104ms	27.83	61.91	107ms	32.98	62.03	109ms
	34B	PIE	30.82	73.84	126ms	42.71	78.94	119ms	51.64	80.15	125ms